Crumpling of a Thin Ice Sheet due to Incident Flow

Toby Wood
Woods Hole Geophysical Fluid Dynamics Program 2008

January 12, 2009

1 Introduction

Consider a sea partially covered by a thin ice sheet, with a prevailing current driving water under the ice edge. If the ice sheet is fixed relative to the flow then a Blasius boundary layer will will develop beneath, due to the no-slip boundary condition at the underside of the sheet. This viscous boundary layer will divert the oncoming flow, causing it to run deeper under the ice, and thus produce a region of high pressure within the fluid in the viscinity of the ice edge. This situation is illustrated in Figure 1. The pressure will cause

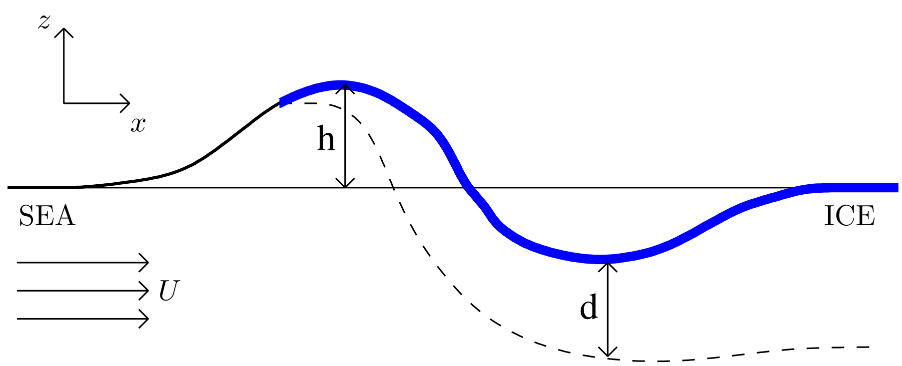

Figure 1: Flow beneath an ice sheet leads to a Blasius boundary layer. The bottom of the boundary layer is indicated by a dashed line.

deformations of both the sea surface and the ice sheet close to the ice edge. If the flow is sufficiently rapid, and the sheet sufficiently thin, then the ice will fracture. Even if the sheet remains intact, it may crumple when the flow speed exceeds some critical value. This crumpling results from a standing flexural wave propagating downstream from the ice edge.

In this report we seek to describe mathematically the deformation of the ice sheet arising from a steady incident flow at the ice edge. (The problem is equivalent to an ice sheet moving across the surface of a stationary fluid.) The formulation of the problem is closely analogous to that employed by Harper & Dixon [3] in their description of the so-called

"Reynolds ridge". In that problem a strong horizontal gradient in surface tension, due to the presence of surfactant contamination, produces an effective no-slip boundary condition beneath the contaminated part of the free surface. Again, a Blasius boundary layer forms, leading to deformation of the free surface. In the present problem, the bending stiffness (or *flexural rigidity*) of the ice sheet replaces surface tension in limiting the curvature of the surface.

There is also an important analogy between the present problem and that of wave scattering by the ice edge, as studied by Balmforth & Craster [1]. In that work, the "forcing" applied to the ice sheet arises from a wave on the sea surface that is incident on the ice edge. No background flow was included, and so there was no Blasius boundary layer — in fact the fluid was regarded as perfectly inviscid. The inclusion of a background flow in the present problem introduces advection terms into the linearised boundary conditions, and so standing waves appear in the solution when the background flow exceeds a critical value.

2 Formulation

Following Harper & Dixon, we regard the Blasius boundary layer beneath the ice sheet as akin to a thin aerofoil; that is, the bottom of the boundary layer represents an inpenetrable barrier to the incompressible fluid flow beneath. Outside the boundary layer we neglect viscous effects, so that the flow may be regarded as irrotational. We may therefore describe the fluid velocity $\mathbf{u}$ in terms of a velocity potential ϕ that satisfies

$$\nabla^2\phi = 0, \tag{1}$$

$$\mathbf{u} = \nabla\phi. \tag{2}$$

The flow upstream is at speed U in the x direction and z is the vertical coordinate relative to the undisturbed free surface. With regard to Figure 1, we take $h(x,t)$ to be the height of the free surface, and $d(x)$ to be the thickness of the viscous boundary layer. If the ice edge is located at $x = 0$ then

$$d(x) = \begin{cases} 0, & \text{for } x < 0 \\ 1.7208\,(\nu x/U)^{1/2}, & \text{for } x > 0 \end{cases} \tag{3}$$

where ν is the kinematic viscosity. Provided that the deflection of the free surface remains small, we may linearise our equations about a state of uniform flow beneath a horizontal free surface. We also suppose that the viscous boundary layer follows the contours of the free surface; this assumption will cease to be valid if the curvature of the free surface becomes comparable to the thickness of the boundary layer [2]. The linearised boundary conditions on the ice surface ($x > 0$) are

$$(\partial_t + U\partial_x)(h - d) = \partial_z\phi|_{z=0} \tag{4}$$

$$(\partial_t + U\partial_x)\phi|_{z=0} + gh = -\frac{B}{\rho}\partial_x^4 h, \tag{5}$$

where ρ is the fluid density and B is the bending stiffness of the ice [5], which is related to the Young's modulus E and Poisson ratio r by

$$B = \frac{E\Delta^3}{12(1-r^2)}. \tag{6}$$

Here, Δ is the thickness of the ice, which we shall assume to be $\approx$ 1m. The characteristic horizontal scale for deformations of the ice surface is the bending length, $L \equiv (B/\rho g)^{1/4}$; for ice of thickness 1m, the bending length is approximately 50m [1].

On the free surface of the open sea, the bending stress vanishes, and in its place we substitute surface tension, σ. We therefore replace (5) with a new dynamic boundary condition for $x < 0$:

$$(\partial_t + U\partial_x)\phi|_{z=0} + gh = +\frac{\sigma}{\rho}\partial_x^2 h. \tag{7}$$

The characteristic horizontal scale on the sea surface is given by the capillary length, $l \equiv (\sigma/\rho g)^{1/2} \approx$ 3mm. Since $l \ll L$ we do not expect surface tension effects to be significant in determining the shape of the ice surface. We have chosen to retain surface tension firstly to regularise any small scale effects occuring on the sea surface. We also have in mind possible laboratory experiments using materials with a much smaller bending length than sea ice, for which surface tension effects would not be negligible.

Due to the discontinuity at the ice edge, we shall need to specify additional "edge conditions" between $x = 0_-$ and $x = 0_+$. In particular, we balance forces and torques at the ice edge by integrating (5, 7) and their first moments across an interval $(-\epsilon, +\epsilon)$, then allowing ϵ to tend to zero. Assuming that $\mathbf{u}$ and h are continuous, we obtain the edge conditions

$$B\partial_x^3 h|_{0_+} = -\sigma\partial_x h|_{0_-} \tag{8}$$
$$B\partial_x^2 h|_{0_+} = -\sigma h|_{0_-}. \tag{9}$$

We now seek two dimensional, steady state solutions of the governing equation (1) subject to (4, 8, 9) and the two-part boundary condition

$$U\partial_x\phi|_{z=0} + gh = \begin{cases} +gl^2\partial_x^2 h, & \text{for } x < 0 \\ -gL^4\partial_x^4 h, & \text{for } x > 0 \end{cases} \tag{10}$$

Following Balmforth & Craster [1], we shall apply the Wiener–Hopf technique, and so we define half-range transforms

$$\Phi_+(k,z) = \int_{0_+}^{+\infty} \phi(x,z)\mathrm{e}^{\mathrm{i}kx}\,\mathrm{d}x \tag{11}$$
$$\Phi_-(k,z) = \int_{-\infty}^{0_-} \phi(x,z)\mathrm{e}^{\mathrm{i}kx}\,\mathrm{d}x \tag{12}$$

The full Fourier transform is then $\Phi = \Phi_+ + \Phi_-$ (similar notation will be employed for the transforms of d and h). With these conventions Φ_+ is well defined (and analytic) in the upper half of the complex k-plane, and Φ_- is similarly well defined in the lower half of

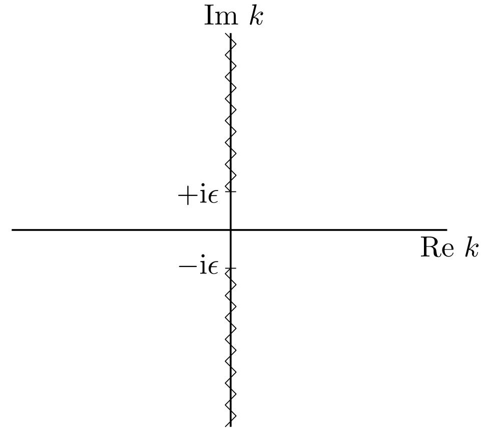

Figure 2: Branch cuts in the complex k plane used in the definition of $\Gamma(k)$.

the complex k-plane. We suppose that Φ_+ and Φ_- can be analytically continued over the complex domains $\oplus$ and $\ominus$, which include, respectively, the upper and lower half k-planes. The full Fourier transform of ϕ (and of h, d, etc.) is then well defined in the intersection[1] of $\oplus$ and $\ominus$. We now transform each of our equations in turn. From (1) we find

$$\begin{aligned} \partial_z^2 \Phi_\pm &= k^2 \Phi_\pm \pm (\partial_x - \mathrm{i}k)\phi|_{0_\pm} && (13) \\ \Rightarrow \partial_z^2 \Phi &= k^2 \Phi && (14) \end{aligned}$$

For simplicity, we restrict attention to the case of deep water. We then have a "lower boundary" condition that $\phi \to 0$ as $z \to -\infty$. The solutions of (14) may then be written as

$$\Phi(k, z) = \hat{\Phi}(k) \mathrm{e}^{\Gamma(k) z}, \tag{15}$$

where $\Gamma(k)$ is defined so that $\Gamma(k) = \pm k$ and $\operatorname{Re}\Gamma(k) \geq 0$. In what follows we shall require a more formal definition of $\Gamma(k)$. We therefore temporarily allow d (and hence ϕ and h) to have some slow sinusoidal modulation in the y direction, with small wavenumber ϵ. Then equation (14) is replaced by

$$\partial_z^2 \Phi = (k^2 + \epsilon^2)\Phi \tag{16}$$

and so $\Gamma(k) = (k^2 + \epsilon^2)^{1/2}$, where we take the branch cuts to lie in the intervals $[\pm\mathrm{i}\epsilon, \pm\mathrm{i}\infty)$ (see Figure 2). The two dimensional problem represents the limiting case in which $\epsilon \to 0$, so we define

$$\Gamma(k) \equiv \lim_{\epsilon \to 0} (k^2 + \epsilon^2)^{1/2}. \tag{17}$$

We now transform the kinematic boundary condition (4) to find

$$\begin{aligned} -\partial_z \Phi_\pm &= \mathrm{i}kU(H_\pm - D_\pm) \pm U(h - d)|_{0_\pm} && (18) \\ \Rightarrow -\Gamma\hat{\Phi} &= \mathrm{i}kU(H - D) && (19) \end{aligned}$$

[1]Formally, the Wiener–Hopf technique requires the intersection of $\oplus$ and $\ominus$ to be some strip containing the real axis. This and other technical details are not addressed here, but are described in detail in [1].

where we have assumed that the boundary layer thickness d is continuous[2] at $x = 0$. Lastly, transforming the two-part dynamic boundary condition (10) yields

$$\begin{aligned} g(1 + L^4k^4)H_+ &= \mathrm{i}kU\hat{\Phi}_+ + gP_{\mathrm{ice}}(k) + U\phi|_{0_+} && (20)\\ g(1 + l^2k^2)H_- &= \mathrm{i}kU\hat{\Phi}_- + gP_{\mathrm{sea}}(k) - U\phi|_{0_-} && (21)\\ \therefore gH + L^4k^4H_+ + l^2k^2H_- &= \mathrm{i}kU\hat{\Phi} + gP(k), && (22)\end{aligned}$$

where

$$\begin{aligned} P_{\mathrm{ice}}(k) &= L^4(\partial_x^3 - \mathrm{i}k\partial_x^2 - k^2\partial_x + \mathrm{i}k^3)h|_{0_+} && (23)\\ P_{\mathrm{sea}}(k) &= l^2(\partial_x - \mathrm{i}k)h|_{0_-} && (24)\\ P(k) &= P_{\mathrm{ice}}(k) + P_{\mathrm{sea}}(k) && (25)\end{aligned}$$

are polynomials in k whose coefficients are the (unknown) values of h and its derivatives at the ice edge. Applying the edge conditions (8–9) we find that

$$P(k) = L^4(-k^2\partial_x + \mathrm{i}k^3)h|_{0_+}, \tag{26}$$

so P is $O(k^2)$ at $k = 0$. We may now eliminate $\hat{\Phi}$ between equations (19) and (22) to obtain a single equation for the free surface:

$$H + l^2k^2H_- + L^4k^4H_+ = \frac{U^2}{g}\frac{k^2}{\Gamma}(H - D) + P. \tag{27}$$

In §3 we shall apply the Wiener–Hopf technique to this equation in order to find $H(k)$ and hence obtain the free surface $h(x)$ via the inverse transform

$$h(x) = \frac{1}{2\pi}\int_{-\infty}^{+\infty} \mathrm{e}^{-\mathrm{i}kx}H(k)\,\mathrm{d}k. \tag{28}$$

Before this, it is instructive to consider two simpler but related problems in which there is no discontinuity in the boundary conditions.

2.1 The Reynolds Ridge

If the boundary condition (7) holds over the entire surface then we replace (27) with

$$H + l^2k^2H = \frac{U^2}{g}\frac{k^2}{\Gamma}(H - D). \tag{29}$$

We now define the Weber number m based on the length scale l

$$m = \frac{U^2}{gl} \tag{30}$$

[2]We have also assumed that $d \to 0$ as $|x| \to \infty$, which is not the case for a Blasius boundary layer. This difficulty can be resolved by introducing a slowly-decaying exponential factor in $d(x)$, then allowing the decay rate to tend to zero.

and the operator

$$\mathcal{D}_{\mathrm{sea}}(k) = 1 + l^2k^2 - mlk^2/\Gamma(k) \tag{31}$$

so that (29) may be written in the form

$$\mathcal{D}_{\mathrm{sea}}(k)H(k) = -mlk^2D(k)/\Gamma(k). \tag{32}$$

We note that $\mathcal{D}_{\mathrm{sea}}(k) = 0$ is the dispersion relation for standing capillary–gravity waves on the free surface:

$$\mathcal{D}_{\mathrm{sea}}(k) \quad = \quad 0 \tag{33}$$

$$\Leftrightarrow (Uk)^2 \quad = \quad g\Gamma(k)(1 + l^2k^2). \tag{34}$$

The full dispersion relation is obtained by replacing $Uk \longrightarrow -\omega + Uk$. The phase and group velocities for capillary–gravity waves are plotted in Figure 3. Provided that there

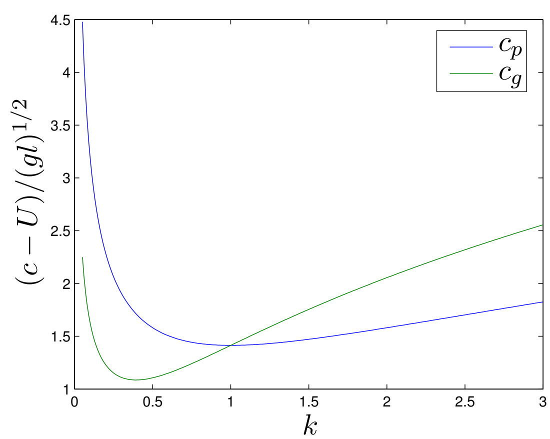

Figure 3: The phase speed c_p and group speed c_g of capillary–gravity waves in a flow of speed U.

are no roots of $\mathcal{D}_{\mathrm{sea}}$ for real k we may readily solve (32) for $H(k)$ and then find the free surface height from (28) by integrating along the real k axis, leading to the solution for the Reynolds ridge problem presented by Harper & Dixon. In general, $\mathcal{D}_{\mathrm{sea}}(k)$ has four complex roots, which we label as k_{s1}, k_{s2}, k_{s3} and k_{s4} according to their location in the complex k-plane (see Figure 4). For $m > 2$ all four roots fall onto the real k axis, corresponding to the existence of standing waves; we must then deform the integration contour in (28) to avoid the singularities in the integrand. The particular choice of integration contour will determine which waves are present as $x \to \pm\infty$, and so we must apply a suitable radiation condition. We see from Figure 3 that the group speed exceeds the phase speed for short wavelength (capillary) waves, and the converse for long wavelength (gravity) waves. We should therefore deform our integration contour so that standing capillary waves appear upstream and gravity waves downstream in the solution [4]. For $x > 0$, the integrand in (28) is exponentially small for Im $k < 0$, so we can close our integration contour at infinity in the lower half k-plane; the solution will only contain waves arising from poles located in the $\ominus$ domain. So we formally regard the two roots of $\mathcal{D}_{\mathrm{sea}}$ with smaller wavenumber k (corresponding to gravity waves) as residing in the lower half k-plane, and label them as k_{s3} and k_{s4}. This leads us to adopt the deformed integration contour shown in Figure 5.

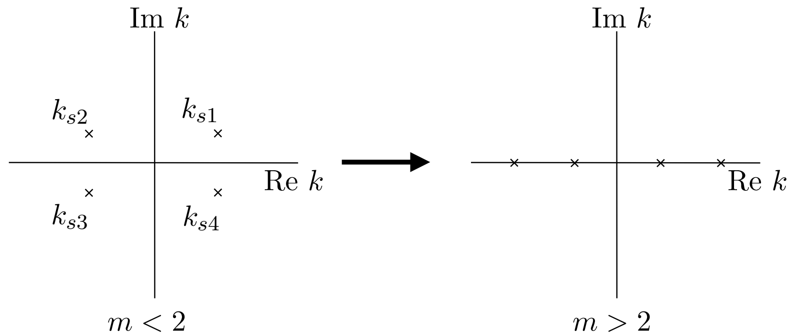

Figure 4: The roots of $\mathcal{D}_{\text{sea}}$ fall onto the real line for $m > 2$.

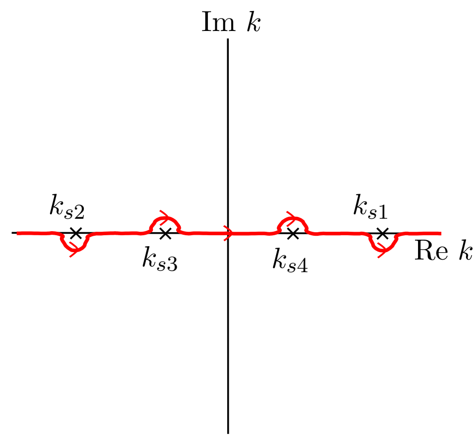

Figure 5: The integration contour used in the inverse transform (28) when $m > 2$.

2.2 Infinite Icesheet

Sufficiently far into the ice covered region we might expect effects from the ice edge to be negligible, and therefore apply boundary condition (5) for all x. In this case, (27) is replaced by

$$H + L^4k^4H = \frac{U^2}{g}\frac{k^2}{\Gamma}(H - D). \tag{35}$$

We proceed by analogy with §2.1; we define a Weber number

$$n = \frac{U^2}{gL} \tag{36}$$

and a dispersion operator

$$\mathcal{D}_{\text{ice}}(k) = 1 + L^4k^4 - nLk^2/\Gamma(k) \tag{37}$$

so that (35) may be written in the form

$$\mathcal{D}_{\text{ice}}(k)H(k) = -nLk^2D(k)/\Gamma(k). \tag{38}$$

$\mathcal{D}_{\text{ice}}(k)$ also has four complex roots, which fall on the real axis when $n > \left(\frac{256}{27}\right)^{1/4} \approx 1.75$; these roots correspond to standing flexural waves on the ice surface. As in the previous section, we must deform our integration contour around these singularities when evaluating the inverse transform (28). Due to the similarities between $\mathcal{D}_{\text{ice}}(k)$ and $\mathcal{D}_{\text{sea}}(k)$, the correct contour is qualitatively identical to that sketched in Figure 5.

3 The Wiener–Hopf Technique

We begin by rewriting (27) in the form

$$\frac{\mathcal{D}_{\text{ice}}}{\mathcal{D}_{\text{sea}}}(k) = \frac{(1+L^4k^4)D - (L^4k^4 - l^2k^2)H_- - P(k)}{(1+l^2k^2)D + (L^4k^4 - l^2k^2)H_+ - P(k)} \tag{39}$$

To proceed with the Wiener–Hopf method we must split the LHS of (39) into a product of $\oplus$ and $\ominus$ functions:

$$\frac{\mathcal{D}_{\text{ice}}}{\mathcal{D}_{\text{sea}}}(k) = -\mathcal{K}_+(k)\mathcal{K}_-(k). \tag{40}$$

The functions $\mathcal{K}_\pm$ must have neither poles nor zeros in their respective domains. We describe the splitting procedure in detail in §A; for now we simply observe that the split is unique up to multiplication of $\mathcal{K}_\pm$ by constants, and that $\mathcal{K}_\pm(k) = O(k)$ as $|k| \to \infty$. We now deduce from (39) that

$$\mathcal{K}_+[(L^4k^4 - l^2k^2)H_+ + (1+l^2k^2)D - P] = \frac{1}{\mathcal{K}_-}[(L^4k^4 - l^2k^2)H_- - (1+L^4k^4)D + P(k)] \tag{41}$$

If $D(k)$ is an entire function then this expression is of the form

$$A_+(k) = A_-(k) \tag{42}$$

where A_+ and A_- are analytic in, respectively, the $\oplus$ and $\ominus$ regions of the complex k-plane. Therefore $A_\pm(k)$ can be extended to an entire function $A(k)$, which is necessarily a polynomial. If, however, $D(k)$ contains finite poles, then these must first be removed. For example, if d is given by

$$d(x,k_0) = \begin{cases} 0, & \text{for } x < 0 \\ 2\sin(k_0x), & \text{for } x > 0 \end{cases} \tag{43}$$

with $k_0 \in \mathbb{R}$ then

$$D(k,k_0) = D_+(k,k_0) = \frac{1}{k+k_0} - \frac{1}{k-k_0}. \tag{44}$$

Since this is a $\oplus$ function, the simple poles at $k = \pm k_0$ must formally be regarded as residing in the lower half plane. We therefore define

$$\begin{aligned} A_+(k,k_0) \;&=\; \mathcal{K}_+\left[(L^4k^4 - l^2k^2)H_+ + \frac{1+l^2k^2}{k+k_0} - \frac{1+l^2k^2}{k-k_0} - P\right] \\ &\quad + \frac{1+L^4k_0^4}{\mathcal{K}_-(-k_0)(k+k_0)} - \frac{1+L^4k_0^4}{\mathcal{K}_-(k_0)(k-k_0)} \end{aligned} \tag{45}$$

$$\begin{aligned} A_-(k,k_0) \;&=\; \frac{1}{\mathcal{K}_-}\left[(L^4k^4 - l^2k^2)H_- - \frac{1+L^4k^4}{k+k_0} + \frac{1+L^4k^4}{k-k_0} + P\right] \\ &\quad + \frac{1+L^4k_0^4}{\mathcal{K}_-(-k_0)(k+k_0)} - \frac{1+L^4k_0^4}{\mathcal{K}_-(k_0)(k-k_0)} \end{aligned} \tag{46}$$

and conclude, as before, that $A_\pm(k,k_0) = A(k,k_0)$, a polynomial in k. The true boundary layer $d(x)$, given by (3), can be written as a superposition of modes of the form (43). In particular,

$$d(x) = \frac{1.7208}{2\sqrt{2\pi}} \left(\frac{\nu}{U}\right)^{1/2} \int_0^\infty \frac{d(x,k_0)}{k_0^{3/2}} \, \mathrm{d}k_0 \tag{47}$$

The free surface $h(x)$ can likewise be written as a superposition of single mode solutions $h(x,k_0)$.

3.1 The single mode solution

We find from (45) and (46) that

$$H_+(k,k_0) = \frac{\frac{1}{\mathcal{K}_+}\left(A(k,k_0) + \frac{1+L^4k_0^4}{\mathcal{K}_-(k_0)(k-k_0)} - \frac{1+L^4k_0^4}{\mathcal{K}_-(-k_0)(k+k_0)}\right) - \frac{1+l^2k^2}{k+k_0} + \frac{1+l^2k^2}{k-k_0} + P}{L^4k^4 - l^2k^2} \tag{48}$$

$$H_-(k,k_0) = \frac{\mathcal{K}_-\left(A(k,k_0) + \frac{1+L^4k_0^4}{\mathcal{K}_-(k_0)(k-k_0)} - \frac{1+L^4k_0^4}{\mathcal{K}_-(-k_0)(k+k_0)}\right) + \frac{1+L^4k^4}{k+k_0} - \frac{1+L^4k^4}{k-k_0} - P}{L^4k^4 - l^2k^2} \tag{49}$$

$$\therefore H(k,k_0) = \frac{-2k_0}{k^2-k_0^2} + \frac{\left(A(k,k_0) + \frac{1+L^4k_0^4}{\mathcal{K}_-(k_0)(k-k_0)} - \frac{1+L^4k_0^4}{\mathcal{K}_-(-k_0)(k+k_0)}\right)\left(\mathcal{K}_-(k) + \frac{1}{\mathcal{K}_+(k)}\right)}{L^4k^4 - l^2k^2} \tag{50}$$

We find from (50) that $H(k,k_0)$ is $O(A/k^3)$ a $k \to \infty$. In order for $h(x)$ to be continuous, $H(k)$ must be $O(1/k^2)$, and so $A(k,k_0)$ must therefore be $O(k)$; we write $A(k) = a(k_0) + b(k_0)k$. The constants a and b are determined by the condition that $H_\pm$ should be analytic for Im $k \gtrless 0$, i.e. that the zeros in the denominators of (48) and (49) must represent removable singularities. Since $P(k)$ is $O(k^2)$ at $k=0$, we therefore require that

$$A(k,k_0) + \frac{1+L^4k_0^4}{\mathcal{K}_-(k_0)(k-k_0)} - \frac{1+L^4k_0^4}{\mathcal{K}_-(-k_0)(k+k_0)} + \frac{1+L^4k^4}{\mathcal{K}_-(k)(k+k_0)} - \frac{1+L^4k^4}{\mathcal{K}_-(k)(k-k_0)} \tag{51}$$

is also $O(k^2)$. This implies that

$$k_0 a(k_0) = -\frac{2}{\mathcal{K}_-(0)} + \frac{1+L^4k_0^4}{\mathcal{K}_-(k_0)} + \frac{1+L^4k_0^4}{\mathcal{K}_-(-k_0)} \tag{52}$$

$$k_0^2 b(k_0) = -2k_0(1/\mathcal{K}_-)'|_0 + \frac{1+L^4k_0^4}{\mathcal{K}_-(k_0)} - \frac{1+L^4k_0^4}{\mathcal{K}_-(-k_0)} \tag{53}$$

For notational convenience, we now define

$$\tilde{A}(k,k_0) \equiv A(k,k_0) + \frac{1+L^4k_0^4}{\mathcal{K}_-(k_0)(k-k_0)} - \frac{1+L^4k_0^4}{\mathcal{K}_-(-k_0)(k+k_0)} \tag{54}$$

$$= -\frac{2}{k_0}\left((1/\mathcal{K}_-)|_0 + (1/\mathcal{K}_-)'|_0 k\right) + \frac{k^2(1+L^4k_0^4)}{k_0^2\mathcal{K}_-(k_0)(k-k_0)} - \frac{k^2(1+L^4k_0^4)}{k_0^2\mathcal{K}_-(-k_0)(k+k_0)} \tag{55}$$

We can now find the free surface height through the inverse transformation (28). In order to evaluate this integral we make use of the fact that

$$\frac{\mathcal{K}_- + 1/\mathcal{K}_+}{L^4k^4 - l^2k^2} = \frac{\mathcal{K}_-}{\mathcal{D}_{\text{ice}}} \tag{56}$$

$$= \frac{-1}{\mathcal{K}_+\mathcal{D}_{\text{sea}}} \tag{57}$$

For $x > 0$, the integrand in (28) decays at infinity for Im $k < 0$. We therefore apply the identity (56) and rewrite equation (50) as

$$H(k, k_0) = \frac{-2k_0}{k^2 - k_0^2} + \tilde{A}(k, k_0)\frac{\mathcal{K}_-(k)}{\mathcal{D}_{\text{ice}}(k)} \tag{58}$$

We calculate $h(x, k_0)$ by collapsing the integration contour in (28) around the branch cut in the lower half plane. In doing so, we pick up pole contributions from the poles at k_{i3}, k_{i4} and $\pm k_0$, all of which are defined as residing in the lower half plane. The solution is

$$h(x, k_0) = -\frac{2nL|k_0|\sin(k_0x)}{1 + L^4k_0^4 - nL|k_0|} + 2\,\text{Im}\left\{\frac{\tilde{A}(k_{i4}, k_0)\mathcal{K}_-(k_{i4})}{4L^4k_{i4}^3 - nL}\text{e}^{-\text{i}k_{i4}x}\right\}$$
$$-\frac{1}{\pi}\int_0^\infty \text{d}\lambda\,\frac{nL\lambda\tilde{A}(-\text{i}\lambda, k_0)\mathcal{K}_-(-\text{i}\lambda)}{(1 + L^4\lambda^4)^2 + n^2L^2\lambda^2}\text{e}^{-\lambda x} \tag{59}$$

The corresponding solution for $x < 0$ is

$$h(x, k_0) = 2\,\text{Im}\left\{\frac{\tilde{A}(k_{s1}, k_0)/\mathcal{K}_+(k_{s1})}{2l^2k_{s1} - nL}\text{e}^{-\text{i}k_{s1}x}\right\}$$
$$+\frac{1}{\pi}\int_0^\infty \text{d}\lambda\,\frac{nL\lambda\tilde{A}(\text{i}\lambda, k_0)/\mathcal{K}_+(\text{i}\lambda)}{(1 - l^2\lambda^2)^2 + n^2L^2\lambda^2}\text{e}^{\lambda x} \tag{60}$$

3.2 The full solution

We deduce from (47) that the free surface height is

$$h(x) = \frac{1.7208}{2\sqrt{2\pi}}\left(\frac{\nu}{U}\right)^{1/2}\int_0^\infty \frac{h(x, k_0)}{k_0^{3/2}}\,\text{d}k_0 \tag{61}$$

Since $\tilde{A}$ is $O(k_0)$ as $k_0 \to 0$ (which can be deduced from (55)), the obvious singularity in (61) is integrable, and the solution is well defined.

4 Results

The effect of the ice edge can be seen by comparing (58) with the solution for an infinite icesheet (38). Indeed we can recover (38) by replacing

$$\tilde{A}\mathcal{K}_- \longrightarrow -(1 + L^4k^4)D \tag{62}$$

in (58). In Figure 6 we illustrate the difference in a particular case. We find, as we might expect on physical grounds, that the presence of the ice edge significantly alters the small scale structure of the solution, but has negligible influence in the limit of zero wavenumber. Both sides of (62) are $-2/k_0 + O(k^2)$ as $k \to 0$.

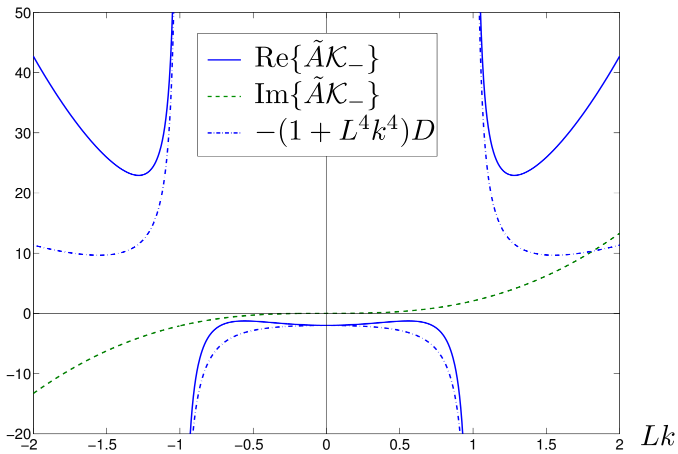

Figure 6: The effect of the ice edge on the single mode solution in the case $k_0 = 1/L$, $n = 1.5$, $l/L = 0.01$. The real and imaginary parts of $\tilde{A}(k, k_0)\mathcal{K}_-(k)$ are shown along with the function $-(1 + L^4k^4)D(k, k_0)$.

A Wiener–Hopf Splitting

We need to find $\mathcal{K}_\pm(k)$ such that

$$\frac{\mathcal{D}_{\text{ice}}}{\mathcal{D}_{\text{sea}}}(k) = -\mathcal{K}_+(k)\mathcal{K}_-(k). \tag{63}$$

To this end, we define

$$\mathcal{R}_{\text{ice}} = \frac{\mathcal{D}_{\text{ice}}(k)}{L^4(k-k_{i1})(k-k_{i2})(k-k_{i3})(k-k_{i4})} \tag{64}$$

$$\mathcal{R}_{\text{sea}} = \frac{\mathcal{D}_{\text{sea}}(k)\Gamma(k)^2}{l^2(k-k_{s1})(k-k_{s2})(k-k_{s3})(k-k_{s4})} \tag{65}$$

Here, k_{ij} and k_{sj} represent the roots of $\mathcal{D}_{\text{ice}}$ and $\mathcal{D}_{\text{sea}}$ lying in the j-th quadrant of the complex k plane. We note that $k_{s2} = -k_{s1}^*$ and $k_{s4} = -k_{s3}^*$ (similarly for the roots of $\mathcal{D}_{\text{ice}}$). The functions $\mathcal{R}_{\text{ice}}$ and $\mathcal{R}_{\text{sea}}$ have only branch cuts in their analytic structure, and tend to unity for large k. Thus we may define

$$\log \mathcal{R}_{\text{ice}}+(k) = \frac{1}{2\pi\mathrm{i}}\int_{-\infty}^{+\infty} \log[\mathcal{R}_{\text{ice}}(k')]\frac{\mathrm{d}k'}{k'-k} \tag{66}$$

$$\log \mathcal{R}_{\text{sea}}+(k) = \frac{1}{2\pi\mathrm{i}}\int_{-\infty}^{+\infty} \log[\mathcal{R}_{\text{sea}}(k')]\frac{\mathrm{d}k'}{k'-k} \tag{67}$$

$$\tag{68}$$

where the integration contour lies below the point $k' = k$. The integrands are continuous provided that we take the branch of the logarithm with a cut along the negative real axis.

The integration contour may then be collapsed around the branch cut in the lower half k' plane, which leads to

$$\log \mathcal{R}_{\text{ice}}\pm(k) = \frac{1}{\pi}\int_0^\infty \tan^{-1}\left[\frac{n\lambda}{1+\lambda^4}\right]\frac{\mathrm{d}\lambda}{\lambda \mp \mathrm{i}Lk} \tag{69}$$

$$\log \mathcal{R}_{\text{sea}}\pm(k) = \frac{1}{\pi}\int_0^\infty \tan^{-1}\left[\frac{n\lambda}{1-l^2\lambda^2/L^2}\right]\frac{\mathrm{d}\lambda}{\lambda \mp \mathrm{i}Lk} \tag{70}$$

Some care is required in choosing the appropriate branches of $\tan^{-1}$ in these expressions. For the first, we require $\tan^{-1} \in [0, \pi)$, but for the second, $\tan^{-1} \in (-\pi, 0]$. This means that the integrand in (70) is $\sim \frac{-1}{\lambda \mp \mathrm{i}Lk}$ as $\lambda \to 0$, implying a logarithmic singularity as $k \to 0$. We may now write

$$\mathcal{K}_+(k) = \frac{L^2(k-k_{i3})(k-k_{i4})}{l(k-k_{s3})(k-k_{s4})}k\frac{\mathcal{R}_{\text{ice}}+(k)}{\mathcal{R}_{\text{sea}}+(k)} \tag{71}$$

$$\mathcal{K}_-(k) = -\frac{L^2(k-k_{i1})(k-k_{i2})}{l(k-k_{s1})(k-k_{s2})}k\frac{\mathcal{R}_{\text{ice}}-(k)}{\mathcal{R}_{\text{sea}}-(k)} \tag{72}$$

We note that $\mathcal{K}_\pm^*(k) = -\mathcal{K}_\pm(-k^*)$ and that $\mathcal{K}_\pm(k) = O(k)$ as $|k| \to \infty$.

References

[1] N. J. Balmforth and R. V. Craster, *Ocean waves and ice sheets*, Journal of Fluid Mechanics, 395 (1999), pp. 89–124.

[2] S. Goldstein, *Modern developments in fluid dynamics*, Oxford University Press, (1938).

[3] J. F. Harper and J. N. Dixon, *The leading edge of a surface film on contaminated flowing water*, Fifth Australasian Conference on Hydraulics and Fluid Mechanics, (1974).

[4] H. Lamb, *Hydrodynamics*, Dover Publications, (1932).

[5] R. D. Mindlin, *Influence of rotatory inertia and shear on flexural motions of isotropic, elastic plates*, Journal of Applied Mechanics, 18 (1951), pp. 31–38.